Extensive grey matter pathology in the cerebellum in multiple sclerosis is linked to inflammation in the subarachnoid space

Owain W. Howell[1, 2]*, Elena Katharina Schulz-Trieglaff[1, 3]*, Daniele Carassiti[1, 4], Steven M. Gentleman[1], Richard Nicholas[1], Federico Roncaroli[1], Richard Reynolds[1]

* joint first authors

[1]Wolfson Neuroscience Laboratories, Centre for Neuroinflammation and Neurodegeneration, Division of Brain Sciences, Imperial College London, UK

[2]Neurology and Molecular Neuroscience, Institute of Life Science 1, College of Medicine, Swansea University, Swansea, SA2 8PP, UK.

[3]Department of Molecules-Signalling-Development, Max Planck Institute of Neurobiology Am Klopferspitz 18, 82152 Martinsried, Germany.

[4]Queen Mary University London, Neurosciences and Neurotrauma, Blizard Institute, London, E1 2AT, UK.

Corresponding author: Professor Richard Reynolds, Division of Brain Sciences, Imperial College Faculty of Medicine, Hammersmith Hospital Campus, Du Cane Road, London W12 00N

r.reynolds@imperial.ac.uk

Tel: 020 7594 6668

Fax: 020 7594 9735

This article has been accepted for publication and undergone full peer review but has not been through the copyediting, typesetting, pagination and proofreading process, which may lead to differences between this version and the Version of Record. Please cite this article as doi: 10.1111/nan.12199

Keywords: Cerebellum, grey matter, meningeal inflammation, multiple sclerosis, demyelination.

Running title: Cerebellum pathology and meningeal inflammation.

Abstract

Aims: Multiple Sclerosis (MS) is a progressive inflammatory neurological disease affecting myelin, neurons and glia. Demyelination and neurodegeneration of cortical grey matter contributes to a more severe disease and inflammation of the forebrain meninges associates with pathology of the underlying neocortical grey matter, particularly in deep sulci. We assessed the extent of meningeal inflammation of the cerebellum, another structure with a deeply folded anatomy, to better understand the association between subarachnoid inflammation and grey matter pathology in progressive MS. **Methods:** We examined demyelinating and neuronal pathology in the context of meningeal inflammation in cerebellar tissue blocks from a cohort of 27 progressive MS cases previously characterized on the basis of the absence/ presence of lymphoid-like aggregates in the forebrain meninges, in comparison to 11 non-neurological controls. **Results:** Demyelination and meningeal inflammation of the cerebellum was greatest in those cases previously characterised as harbouring lymphoid-like structures in the forebrain regions. Meningeal inflammation was mild to moderate in cerebellar tissue blocks and no lymphoid-like structures were seen. Quantification of meningeal macrophages, CD4+, CD8+ T lymphocytes, B cells and plasma cells revealed that the density of meningeal macrophages associated with microglial activation in the grey matter, and the extent of grey matter demyelination correlated with the density of macrophages and plasma cells in the overlying meninges, and activated microglia of the parenchyma. **Conclusions:** These data suggest that chronic inflammation is widespread throughout the subarachnoid space and contributes to a more severe subpial demyelinating pathology in the cerebellum.

List of abbreviations used

F-, absence of lymphoid-like aggregates; F+, presence of lymphoid-like aggregates ; GM, grey matter; GML, grey matter lesion; NAGM, normal appearing grey matter; ROI, region of interest; SPMS, secondary progressive multiple sclerosis; WM, white matter.

Introduction

Subpial grey matter (GM) pathology is a hallmark of the progressive stages of MS and associates with inflammatory infiltration of the overlying meninges (1). Recent studies of cortical biopsies have shown that GM demyelination and accompanying meningeal inflammation may also be a major feature of from the earliest stages of MS (2). Lesions of the GM are found in the spinal cord, cerebellum, midbrain and neocortex and are thought to account for many of the complex symptoms of the disease, including deficits in cognition, disturbances of mood, and an increased risk of seizures, fatigue and motor disability (3,4).

The cerebellum is often severely affected in MS patients and cerebellar demyelination and atrophy can occur early in the course of the disease (5–7). Cerebellar ataxia and tremor are predictive of a more severe clinical course (8) and MS patients with severe cerebellar pathology have distinct cognitive deficits (9,10). MRI studies that analysed cerebellar volume in MS patients showed that the GM is more extensively affected than the white matter (WM). Although SPMS cases exhibit the greatest pathology (6), significant atrophy is also seen in patients with relapsing remitting disease and patients with clinically isolated syndrome (11). Changing cerebellar cortical volume, cerebral volume and age are the best predictors of conversion from a relapsing remitting to a secondary progressive clinical course (12). These findings indicate an important role for cerebellar pathology in all stages of the disease. Post-mortem studies have confirmed the extensive cerebellar demyelination in progressive MS and in particular, the predilection for the GM (13,14), but the relationship between the demyelination and degree of inflammation has not been investigated.

Increased meningeal inflammation, consisting of CD4+ and CD8+ T-cells, B-cells, macrophages and plasma cells, is characteristic of progressive MS and has been associated with underlying cortical pathology (15–17), especially subpial lesions, which are often located in deep sulci and can also span several gyri (18,19). The presence of a high number of lymphocytes in the cerebral meninges of MS patients (20–22), together with the almost complete lack of infiltrating lymphocytes in chronic lesions of the GM (19), has led to the hypothesis that the meningeal compartment might be a source of a pathogenic factor or factors affecting the underlying brain tissue (17,23) and may sustain chronic inflammatory pathology in long-standing disease.

Due to the relationship between both diffuse inflammation and organised lymphoid-like infiltrates in the meninges and the underlying subpial cortical pathology associated with deep sulci (15,17,24,25), we have investigated this relationship in the cerebellum, given its deeply folded anatomy. Here we ask whether MS cases characterized by increased forebrain meningeal and perivascular inflammation have a corresponding elevated cerebellar meningeal inflammation and does this meningeal inflammation associate with a greater pathology of the underlying cerebellar cortical tissue. Through this quantitative study of inflammation, demyelination and neurodegeneration, we strengthen the hypothesis that in the progressive phase of MS, diffuse inflammation of the subarachnoid compartments of the brain and cerebellum influences the underlying WM and GM pathology and that this contributes to a more severe disease.

Materials and Methods

Tissue selection

All tissue was provided by the UK MS Society Tissue Bank at Imperial College, London. Tissue was obtained via a prospective donor scheme with full ethical approval by the National Research Ethics Committee (08/MRE09/31). Clinical data was reviewed and collated by a senior neurologist with a specialist interest in MS (RN) and details of age of onset, age of progression, age of wheelchair use

and age of death reported. Case selection was based on a previous cohort of cases that were extensively characterised and divided into those exhibiting lymphoid-like cellular aggregates in the cerebral meninges (F+SPMS) and those without (F-SPMS) (24). Of the 27 selected cases, 14 had whole fixed cerebellum available. Post-mortem delay did not differ significantly between SPMS and control cases (SPMS, 25.7± 4hrs; Control, 21.5±4.1hrs; p=0.3; table 1). Individual patient data is summarised in supplementary table 1.

Tissue preparation and block selection

Post-mortem tissue was fixed in 4% paraformaldehyde in phosphate buffered saline (PBS), dehydrated and embedded in paraffin wax under vacuum. Sagittal sections from tissue blocks (2x2x1cm) of cerebellum, taken 1cm lateral to the midline and including the dentate nucleus, were used for quantitative measurements of inflammatory and neuronal pathology. One block per case and a maximum of four areas of interest per section (two in GM lesions [GML], two in the normal grey matter [NAGM]), were analysed by immunohistochemistry. Axial hemispheric or bi-hemispheric cerebellar sections (prepared at the level of the horizontal fissure) from fourteen cases (supplementary table 1) were used for assessment of the gross extent of WM and GM demyelination (to supplement the small cerebellar block analysis), but were not suitable for quantitative measures of inflammation due to the difficulty in preservation of the meningeal tissue regions of interest in all samples for all immune cell markers assessed.

Semi-quantitative analysis of inflammation

Sections from small blocks of cerebellar cortex and dentate nucleus were stained with haematoxylin and eosin (H + E) and a semi-quantitative assessment of inflammation in the meninges was performed (24). Only cases with cut sections containing well preserved leptomeninges were used in this study. The cases were divided into four groups, 0+, +, ++, and +++, based on the degree of

meningeal inflammation. Group 0+ exhibited no, or very mild, aggregates of inflammatory cells (less than 10 cells in the largest aggregate); + cases showed moderate (10-30 cells) inflammation; ++ cases revealed at least a single infiltrate of >30 cells, which were loosely clustered. Cases presenting with at least one dense and compact aggregate of >100 cells were rated +++, (see Fig. 1A-D).

Immunohistochemistry

Six µm thick serial sections were cut from wax-embedded small blocks or from hemispheric horizontal macroblocks and immunohistochemical staining was performed as described previously (24). Primary antibodies used are summarised in table 2. All immunolabelled sections were counterstained with haematoxylin before dehydration, clearing in xylene and coverslipping in DePeX (VWR International).

Quantitative analysis of demyelination

For quantification of demyelination, sections of cerebellum and whole cerebellar bihemispheric and hemispheric sections were stained for myelin oligodendrocyte glycoprotein (MOG)/haematoxylin and analysed microscopically (200-400x magnification). Following immunochemistry, sections were scanned at 1200 dpi using a conventional flat-bed scanner and WM and GM demyelinating lesions demarcated as colour masks using Photoshop CS5 (Adobe Systems Incorporated, California, USA), with the stained slides as reference. Deep WM and GM, such as the dentate nucleus and the brainstem, were not included in the analysis, since blocks contained differing proportions of these structures. The area of colour depicting demyelinated or normal-appearing WM or GM was measured in pixels (ImageJ, NIH image), and the mean percent WM, GM and total cerebellar (excluding deep WM) demyelination compared between cases and between groups.

Regions of interest for analysis of inflammation and neurodegeneration

GML percentages in small blocks of cerebellum correlated significantly with the same measures in whole and hemispheric blocks, from the fourteen cases in which these comparisons could be made (Spearman r=0.68, p= 0.0077).This indicated that measures of demyelination in cases where only small blocks of cerebellum where available served as a reliable measure of global cerebellum pathology. Two regions of interest (ROI) per GML, NAGM and per accompanying overlying meninges were chosen from the MOG stained small blocks for each case. ROI were defined based on pathology and location, with all GML and NAGM lying at the margins and not the base of the cerebellar sulci, and all containing intact meninges (Fig. 2A). Only GML ROI bounded by normal appearing white matter were analysed to ensure consistency in lesion selection between cases.

Quantitative analysis of inflammation and neurodegeneration

For all assessments, a maximum of four 200x images (area of one image: 0.187 mm^2) per ROI were captured, with a maximum of eight ROI per case, dependent on available GML (i.e. two NAGM ROI, two of accompanying meninges plus 2 GML ROI and 2 of overlying meninges). CD68+, CD20+, CD4+, CD8+ and immunoglobulin A, G and M+ (Ig+) inflammatory cells in all intact meninges, excluding those cells within the confines of vessels, were counted and data expressed as cells per unit length (mm or cm) of intact meninges. Parenchymal inflammation and neurodegeneration were assessed in the molecular and granule cell layers. To ensure a comparable depth of parenchyma was sampled in each case, the Purkinje cell layer (PCL) was laid horizontally and mid-way across the image before digital capture. Macrophage/microglial density in the GM parenchyma, excluding those of the perivascular or vascular space, was evaluated by quantifying CD68+ cells (expressed as cells per mm^2 of GM). Purkinje cell (PC) number and morphology was evaluated by immunostaining for non-phosphorylated neurofilaments. For this, a minimum of 10 images per ROI, and a maximum of two ROI´s per block (one in GML and one in NAGM) per case were captured. PC densities were expressed as cells per mm of PCL. In order to assess PC morphology, the circumference and area of the cell soma were measured and the *f*-value of circularity determined (26). A minimum of 10 cells per

normal or lesioned ROI that exhibited a clear nucleolus were analysed. The intensity of anti-synaptophysin immunoreactivity in the granule cell layer (GCL) and the molecular layer (ML) were quantified as areas of positive immunostaining above a manually adjusted threshold (ImageJ). Synaptophysin immunoreactivity measures were corrected for background signal by subtracting the mean intensity anti-synaptophysin signal in the WM of each quantified section. The area of calbindin positive neurites of the molecular layer (ostensibly a measure of Purkinje cell dendrite density) was calculated as a fraction of the area of the total molecular layer sampled.

Image analysis and quantification

Images were viewed and captured using a Leica DM 2500 microscope (Leica Microsystems, Bucks, UK) connected to a MicroPublisher 3.3 RTV digital camera (QImaging, Staffordshire, UK). Quantification of inflammatory cells and neurodegeneration was accomplished with ImageJ manual tag and area/ length measures tools. Images were prepared for publication with Photoshop CS5. All quantifications were performed with the researcher blinded to case number and disease/control status.

Statistical analysis

Data was collated in Excel (Microsoft Office 2007) and analysed using GraphPad PRISM 6 (GraphPad Inc., California, and USA). Results were expressed as the mean +/- standard error of the mean (SEM) or as median +/- interquartile range (IQR) and analysed using the appropriate parametric (ANOVA and Bonferroni's multiple comparison post-test) or non parametric tests (Kruskal-Wallis and Dunn's multiple comparison post-test or the Mann-Whitney U-test), as stated in the legends. Associations between independent variables per case were compared by non-parametric Spearman's Rank correlation analysis.

Results

Multiple sclerosis cases with lymphoid-like structures in the cerebral meninges exhibited greater demyelination in both the cerebellar white and grey matter

We first quantified the extent of demyelination in the GM and WM of the cerebellum in a previously characterised cohort of SPMS cases characterised by the presence of lymphoid follicle-like (F+, n=12) or the absence of lymphoid follicle-like (F- n=15) structures in the forebrain (24). Myelinated fibres in the normal cerebellar GM are found predominantly in the granule cell layer with only small numbers in the molecular layer just above the Purkinje cells (Fig. 1A, B). Demyelination of the GM was widespread (Fig. 1A, arrowheads), with one or more cerebellar folia affected (Fig. 1C, D), most notably surrounding deep folds (Fig. 1A). Cerebellar demyelination was assessed by overlaying digital images with a colour mask to highlight microscopically confirmed WM and GM lesions (Fig. 1E-H). WM pathology was rarely seen in the absence of topographically associated GM lesions, whereas the converse was often the case (Fig. 1D), suggesting that the extension of GM subpial pathology into the WM is a common feature of cerebellar lesions. GM demyelination was far more extensive than WM pathology in the SPMS cases displaying demyelinating pathology (percent area white matter lesion of total WM: 3.04% (IQR 0.91- 14.9%); percent area grey matter lesion of total GM: 14.23% (3.17- 37.42%); p=0.016). In extreme cases (Fig. 1H; MS217)), almost the entire GM was demyelinated, whilst the WM was largely spared. Demyelination of the GM (32.04% (13.5- 83.25%) and 10.3% (2.4- 16.39%); p=0.03), the WM (10.31% (2.29- 22.58%) and 2.35% (0.85- 4.8%); p=0.048) and total GM and WM (27.2% (8.84- 61.91%) and 9.3% (3.0- 21.52%); p=0.04) was significantly greater in F+SPMS than in the F-SPMS cohort, respectively (Fig. 1I). Out of the fourteen cases with available whole cerebellar macroblocks (supplementary Table 1), twelve (n=5 F-SPMS, n= 7 F+ SPMS) had matching whole forebrain coronal sections previously used to measure cortical demyelination (24). We found there to be a significant association between the extent of subpial GM demyelination in the forebrain

and cerebellum (Fig. 1J), suggesting that common mechanisms may influence the extent of subpial demyelination in these areas.

Meningeal inflammation is elevated in cases harbouring lymphoid-like aggregates in the forebrain meninges

The finding that cases previously characterised as F+SPMS displayed greater demyelinating pathology of the cerebellum, and particularly more extensive subpial demyelinating pathology, led us to investigate the nature and extent of inflammatory cell infiltration of the cerebellar meninges. We found cellular infiltration of the cerebellar meninges to be moderate and increased compared to control (median rating: control 0+, SPMS +; $p< 0.0001$) (Fig. 2A-D). The majority of cases rated without lymphoid-like structures in the forebrain (F-SPMS) were rated 0+ or + (F-: 0+ 3/15; + 11/15; ++ 1/15), whereas cases with lymphoid-like structures in the forebrain (F+SPMS) were mostly assigned to the + and ++ groups (F+: + 7/12; ++ 4/12; +++ 1/12, $p=0.011$). Only one F+SPMS case (MS257) displayed extensive (+++) immune cell aggregates in the cerebellar meninges (Fig. 2E-G). Further immunostaining of one of these (+++) aggregates for CD20, CD3 and immunoglobulins revealed a B-cell rich aggregate core surrounded by T-cells and numerous plasma cells in a small lymphoid-like structure. We were unable to further characterise the cellular composition of this structure to confirm or reject its status as a bona-fide lymphoid-like aggregate (e.g. the presence of CD35+ follicular dendritic cells and Ki67+/CD20+ B-cells (17,22)) due to the loss of the area of interest from subsequent sections. An example of a (++) rated inflammatory infiltrate from an F- case is shown (MS395; Fig. 2H-I). The semi-quantitative analysis revealed that the degree of cerebellar meningeal inflammation is related to the degree of forebrain inflammation ($r= 0.59$, $p=0.0012$ comparing semi-quantitative ratings of maximum meningeal immune cell infiltrates in blocks of cerebellum and neocortex per case, n=27 cases). In contrast to that seen in forebrain meninges (24), inflammation of the cerebellar meninges was mild to moderate and lymphoid-like structures were not detected.

Characterisation, quantification and clinical associations of meningeal inflammation in SPMS cerebellum

B cells and plasma cells: CD20+ B-cells and immunoglobulin A+, G+, M+ plasma cells (Ig+) were distributed throughout the cerebellar meninges (Fig. 2, 3). The number of CD20+ B cells per cm of intact meninges (Fig. 3A, B) was not significantly increased in SPMS versus region matched controls (p=0.152, Mann-Whitney U-test), although separate analysis of the F+SPMS cohort (Fig. 3B) demonstrated a 3-fold increase in B-cell numbers compared to controls (p=0.0091), and a 1.7-fold increase (p=0.015) compared to F- cases. The number of meningeal Ig+ plasma cells was significantly elevated in SPMS (control 6.5 (3.58- 13.56) cells/cm and SPMS 12.32 (7.88- 19.3) cells/cm; p=0.011, Mann-Whitney U-test), with F+SPMS (p=0.029) and F- SPMS (p=0.015) median values differing significantly to controls (Fig. 3C). No CD20+ B-cells or Ig+ plasma cells were seen in the cerebellar parenchyma of SPMS or control cases.

CD68+ monocytes/macrophages: CD68+ monocytes/macrophages were abundant in the cerebellar meninges (Fig. 2E), and constituted the largest proportion of inflammatory cells in this compartment (control= 13.68 (13.31- 14.55) cells/mm, SPMS= 22.68 (17.49- 28.71) cells/mm, p<0.0001, Mann-Whitney U-test). Sub-group analysis demonstrated CD68+ cells to be enriched in both F+SPMS and F- SPMS cases compared to controls (Fig. 3D).

CD4+ and CD8+ T lymphocytes: Scattered T-cells were observed throughout the subarachnoid space overlying the cerebellar folia. The number of meningeal CD4+ cells (Fig. 3E), but not the number of CD8+ T-cells (Fig. 3F), was significantly increased in SPMS cases in comparison to controls (Control CD4+ T-cells/mm= 1.83 (1.20- 2.61), SPMS CD4+ cells/mm= 3.02 (1.93- 4.78), p=0.0223, Mann-Whitney U-test). The density of CD4+ T-cells was elevated in F+ SPMS in comparison to both control and F- SPMS (Fig. 3E).

Lymphoid-like positive SPMS cases exhibited greater microglial activation in the cerebellar grey matter

Our quantification of inflammatory cells revealed a modest, but significant, rise in the number of inflammatory cells in the cerebellar meninges. In order to better understand the role of parenchymal inflammation in cerebellar pathology, we quantified the density of CD68+ cells with a microglial/ macrophage phenotype in the cerebellar GM. In general, CD68+ microglia/macrophages were abundant in both the WM and the GM, and were present in elevated numbers in both the granule cell and molecular layers of SPMS in comparison to controls (Fig. 4). Of note was the topographical association seen between increased CD68+ inflammation of the subarachnoid space and elevated density of CD68+ microglia/macrophages of the molecular and Purkinje cell layers in SPMS (Fig. 4B, D). A statistically significant (p=0.031) increased density of CD68+ cells was observed in the SPMS cases (114.7 (79.02- 138.0) cells/ mm^2) in comparison to controls (90.85 (82.83- 110.4) cells/ mm^2, Mann-Whitney U-test), which was attributable to the significantly increased density of parenchymal CD68+ cells in the F+ cases (Fig. 4C). No difference was seen between the density of CD68+ parenchymal inflammation in the GML and NAGM (data not shown), reflecting the chronic nature of the GM lesions in these cases.

Inflammation of the cerebellar meninges associates with more extensive parenchymal pathology

We performed correlation analysis to investigate the association between inflammation and underlying demyelination in the cerebellum (Table 3). The number of CD68+ meningeal macrophages (cells/mm) correlated with the density of total T-cells (CD4 and CD8; Spearman r= 0.6, p= 0.00021), with CD4+ T-cells (p= 0.031), and with CD20+ B-cells (p= 0.0322). Spearman analysis revealed that the density of CD68+ macrophages of the cerebellar meninges correlated modestly with the density of activated microglia (p= 0.007). Parenchymal microglial/macrophage activation correlated with the degree of grey matter demyelination (p= 0.0451) and the density of Ig+ plasma cells associated with the extent of GML (p= 0.031).

Clinical features are associated with greater demyelination in both the cerebellar white and grey matter

We determined whether any clinical features (supplementary table 1) were associated with an increased extent of demyelination in the cerebellum . We found that active disease at the time of death was modestly associated with increased total lesion area (r= 0.31, p<0.008), white matter lesion area (r= 0.24, p<0.02) and grey matter lesion area (r= 0.31, p<0.008, Spearman's Rank correlation analysis in all instances).

Meningeal inflammation was not associated with significant Purkinje cell degeneration

Immunohistochemical staining for non-phosphorylated neurofilaments was used to identify PCs of the normal appearing and demyelinated GM (Fig. 5). Quantification revealed no significant difference in the PC density between controls and the SPMS, or between controls and F- and F+ cohorts (controls 6.0±1.4 cells/mm, F-SPMS 5.6±1.9 cells/mm, F+SPMS 4.9±1.5 cells/mm), although a trend to a reduced density of PCs in cases with greatest forebrain inflammation could be seen (p= 0.068; Fig 5B). Measures of PC circularity, which is often taken as an indication of neuronal stress, did not reveal any differences between the three cohorts (controls 0.851±0.03; F-SPMS 0.852±0.02, F+SPMS 0.852±0.04). The density of non-phosphorylated neurofilaments/calbindin-positive neurites was also unchanged (data not shown), but evidence of PC axon pathology was noted (Fig. 5C). No difference in total granule cell/molecular layer synaptophysin staining density was seen (F+SPMS 22.1±9.0, F-SPMS 24.1±8.8, controls 18.5±8.6; Kruskal Wallis and Dunn's post test; Fig. 5D) or between granule cell or molecular cell layers when analysed separately (p>0.2 in all instances, Kruskal Wallis and Dunn's post test), which is in agreement with previous work (14). No associations between the density of synaptophysin staining and variables known to effect immunoreactivity, such as the time from death

to tissue processing (P> 0.5) or the time in fixative (P> 0.5, Spearman's Rank analysis), were observed.

Discussion

In this study we have demonstrated that cases of SPMS exhibiting an increased meningeal inflammation are characterized by greater GM and WM demyelination in the cerebellum. The diffuse nature of the inflammation supports the hypothesis of the subarachnoid space of the meninges as a source of cells and soluble factors capable of mediating widespread cerebral and cerebellar demyelinating pathology.

In agreement with previous studies (13,14), we documented extensive cerebellar demyelination and have shown that the proportion of demyelinated GM far exceeded that of the subcortical WM. GM lesions often encompassed multiple folia, extended into the granule cell layer and were most extensive in cases characterized by meningeal inflammation and an active disease course at death. This result is similar to findings in the neocortex where subpial lesions predominate (17,19,21,24). The lack of topographical association between GM and WM plaques and the finding that GML volume and WML volume in individuals are independent of each other (13), may argue for a different pathogenesis of GM and WM lesions during progressive MS. We believe these differences in WM and GM pathology may in part be due to the close proximity of the GM to the inflammatory milieu in the overlying meninges. In fact, meningeal inflammation associates more widely with underlying GM damage of the forebrain and cerebellar cortices, where the extent of pathology may be fundamental to disease progression (12).

We report a significant increase in CD20+ B-cells, CD4+ T-cells and CD68+ macrophages in the meninges of the cerebellum in SPMS cases that have significant forebrain infiltrates and lymphoid -

like structures. Increased connective tissue inflammation, in combination with the associated increased density of activated microglia in the underlying cerebellar cortex, might contribute to the increased GM pathology of F+ cases, in comparison with those cases displaying less meningeal inflammation. When compared with the extent of inflammation of the cerebral cortex, the degree of cerebellar subarachnoid inflammation was mild to moderate, being some 2-3-fold greater than that in region matched control samples. Analysis of forebrain samples in cases of SPMS and primary progressive MS revealed subarachnoid inflammation to be substantially greater than controls (15,24) and suggested that the extensive demyelination observed in the cerebellar GM in SPMS is likely to be caused by a toxic CSF milieu, which is partly independent of detectable inflammatory infiltrates in the tight confines of the cerebellar subarachnoid space. We did not detect lymphoid-like aggregates in the cerebellar meninges and speculate their absence reflects the modest meningeal cell inflammation in the space-limited confines of the cerebellar sulci. This environment may not be conducive to the formation of organised lymphoid-like structures, which are most frequently seen in the large sulci of the cingulate, insular and temporal regions of the forebrain (24). We suggest that the presence of cytotoxins reflects the chronic and compartmentalised neuroinflammatory response of long standing disease, which is linked to subpial myelin pathology (27). It should be appreciated, given the varied extent of meningeal and parenchymal pathology in our study cohort that other pathogenetic mechanisms, such as neuronal and axonal pathology secondary to distant lesions, are also contributing to cerebellar damage.

The number of CD68+ macrophages in the cerebellar meninges greatly exceeded other inflammatory cells and correlated with parenchymal microglial activation. These findings are in keeping with previous studies showing an association between meningeal cellular infiltrates and parenchymal microglial/macrophage activation in the forebrain (15,24,28), which hitherto had not been previously demonstrated in the cerebellum (14). This and other studies support a key role for activated microglia (CD68+) as effectors of myelin damage, although these cannot be the sole drivers of

pathology given that activated microglia are a feature of non-demyelinating chronic diseases of the CNS (28). Plasma cells have been shown to be enriched in MS cases compared to other inflammatory neurological disorders (29), and CNS expanded pools of plasmablasts secrete intrathecal immunoglobulins (30). We show a significantly increased number of plasma cells in all SPMS cases and a correlation between the numbers of meningeal plasma cells with the area of demyelinated grey matter, suggesting that their role as antibody producing cells is likely to contribute to the extensive demyelination of the cerebellum, in concert with the resident activated microglia. A role for pathogenic antibodies in the genesis of cortical lesions has not been demonstrated histopathologically, although immunoglobulin gene expression is deregulated in cortical MS lesions (31) and intrathecal immunoglobulin levels associate with cortical lesion load in clinically isolated syndrome (32). Our study found that the number of B-cells and CD4+ T-cells were increased in F+SPMS only, albeit at very low numbers relative to the number of macrophages, and suggests key effector functions for these cells in augmenting myelin pathology in the F+ SPMS group. An increasingly appreciated antibody-independent function of B-cells as a dynamic antigen presenters, a source of inflammatory cytokines and prerequisite for self-reactive T-lymphocyte responses is being revealed (33,34). Patient derived B-cell cytokines/chemokines have been shown to mediate oligodendrocyte and glial pathology in vitro (35). Intrathecally derived B-cell populations can also be seen in clinically isolated syndrome and relapsing remitting MS and associate with more severe disease progression (36), whilst clinical and experimental data derived from use of the B-cell depleting humanised monoclonal antibody to CD20 has been key to the reappraisal of the role of CD20+ B-lymphocytes in CNS autoimmunity (37,38).

Cerebellar dysfunction is a significant prognostic factor for a poor disease outcome in patients with MS (39) and it is closely correlated with signs of disability, such as ataxia, tremor and nystagmus (8). Our finding that GML are more frequent, and account for a greater area of the affected cerebellum than do white matter lesions, suggests that GML are contributory to sjgns and symptoms of

cerebellar dysfunction in secondary progressive MS (13,14). Neuroaxonal changes may contribute to clinical features, but we were unable to detect any significant changes in cell number or morphology, or the density of neurites or synapses. Quantification of individually stained synaptophysin+ boutons by stereology may be necessary to detect these more subtle changes (40). Purkinje cells seem to persist in remarkably high numbers in the cerebellum of long-standing MS (14), which may in part be protected by processes of nuclear fusion (41) or be a reflection of the lower grade of connective tissue inflammation found in the tight confines of the cerebellar subarachnoid tissue, which contrasts with the significant forebrain inflammation and associated loss of the pyramidal cells of the motor cortex (25). Other changes in Purkinje cells, including the altered expression of ion channels, may cause dysfunction of cerebellar neural networks and contribute to the cerebellar symptoms of disease without significant neurodegeneration (42).

Conclusions

Subpial demyelinating lesions are a pathological feature exclusive to MS (43) and meningeal inflammation associates with subpial lesions in acute MS and in progressive disease (2,17), with a gradient of cortical tissue damage (25) and inflammatory infiltrates of the meninges that correlate with the severity of the clinical course (24). Our description of the presence of both meningeal inflammation and extensive GM subpial demyelinating pathology in the cerebellum suggests that regions with a deeply folded anatomy serve as a reservoir of inflammatory cells and cytokines in areas of restricted CSF flow. This work serves to highlight the important consideration that should be given to targeting this persistent central inflammation in order to inhibit the progressive course of MS.

Acknowledgements

Work described in this study was funded by the Multiple Sclerosis Society (Grant No. 910/09 to RR, FR, RN, SG), the Medical Research Council (Grant No. G0700356 to RR, OH) and, in part, by the European Union's Seventh Framework Program (FP7/2007-2013) under grant agreement no. HEALTH-F2- 2011-278850 (INMiND) to FR. Human tissues were provided by the UK MS Society Tissue Bank at Imperial College London.

Author contributions

OH, RR- designed the study; OH, EKST, DC- prepared sections, performed immunostaining and quantitative morphometry; SG, RN, FR- provided neuropathological, clinical and demographic summaries for all cases; OH, EKST,RR- wrote the manuscript with input from all authors.

Conflict of interest statement

The authors report no conflict of interest.

References

1. Reynolds R, Roncaroli F, Nicholas R, Radotra B, Gveric D, Howell O. The neuropathological basis of clinical progression in multiple sclerosis. Acta Neuropathol 2011;122(2):155–70.

2. Lucchinetti CF, Popescu BFG, Bunyan RF, Moll NM, Roemer SF, Lassmann H, Brück W, Parisi JE, Scheithauer BW, Giannini C, Weigand SD, Mandrekar J, Ransohoff RM. Inflammatory cortical demyelination in early multiple sclerosis. N Engl J Med 2011;365(23):2188–97.

3. Geurts JJG, Barkhof F. Grey matter pathology in multiple sclerosis. Lancet Neurol 2008; 7(9):841–51.

4. Pirko I, Lucchinetti CF, Sriram S, Bakshi R. Gray matter involvement in multiple sclerosis. Neurology. 2007;68:634–42.

5. Crespy L, Zaaraoui W, Lemaire M, Rico A, Faivre A, Reuter F, Malikova I, Confort-Gouny S, Cozzone PJ, Pelletier J, Ranjeva JP, Audoin B. Prevalence of grey matter pathology in early multiple sclerosis assessed by magnetization transfer ratio imaging. PLoS One 2011;6(9):e24969.

6. Anderson VM, Fisniku LK, Altmann DR, Thompson AJ, Miller DH. MRI measures show significant cerebellar gray matter volume loss in multiple sclerosis and are associated with cerebellar dysfunction. Mult Scler 2009; 15(7):811–7.

7. Calabrese M, Mattisi I, Rinaldi F, Favaretto A, Atzori M, Bernardi V, Barachino L, Romualdi C, Rinaldi L, Perini P, Gallo P. Magnetic resonance evidence of cerebellar cortical pathology in multiple sclerosis. J Neurol Neurosurg Psychiatry 2010;81(4):401–4.

8. Weinshenker BG, Rice GP, Noseworthy JH, Carriere W, Baskerville J, Ebers GC. The Natural History of Multiple Sclerosis: A Geographically Based Study. 3. Multivariate analysis of predictive factors and models of outcome. Brain 1991;114(2):1045–56.

9. Cerasa A, Valentino P, Chiriaco C, Pirritano D, Nisticò R, Gioia CM, Trotta M, Del Giudice F, Tallarico T, Rocca F, Augimeri A, Bilotti G, Quattrone A. MR imaging and cognitive correlates of relapsing-remitting multiple sclerosis patients with cerebellar symptoms. J Neurol 2013; 260(5):1358-66.

10. Valentino P, Cerasa A, Chiriaco C, Nisticò R, Pirritano D, Gioia M, Lanza P, Canino M, Del Giudice F, Gallo O, Condino F, Torchia G, Quattrone A. Cognitive deficits in multiple sclerosis patients with cerebellar symptoms. Mult Scler 2009;15(7):854–9.

11. Ramasamy DP, Benedict RHB, Cox JL, Fritz D, Abdelrahman N, Hussein S, et al. Extent of cerebellum, subcortical and cortical atrophy in patients with MS: a case-control study. J Neurol Sci;282(1-2):47–54.

12. Calabrese M, Romualdi C, Poretto V, Favaretto a, Morra a, Rinaldi F, Minagar A, Dwyer MG, Zivadinov R. The changing clinical course of multiple sclerosis: A matter of grey matter. Ann Neurol 2013; 74(1):76-83.

13. Gilmore CP, Donaldson I, Bö L, Owens T, Lowe J, Evangelou N. Regional variations in the extent and pattern of grey matter demyelination in multiple sclerosis: A comparison between the cerebral cortex, cerebellar cortex, deep grey matter nuclei and the spinal cord. J Neurol Neurosurg Psychiatry 2009;80(2):182–7.

14. Kutzelnigg A, Faber-Rod JC, Bauer J, Lucchinetti CF, Sorensen PS, Laursen H, Stadelmann C, Brück W, Rauschka H, Schmidbauer M, Lassmann H. Widespread demyelination in the cerebellar cortex in multiple sclerosis. Brain Pathol 2007;17(1):38–44.

15. Choi SR, Howell OW, Carassiti D, Magliozzi R, Gveric D, Muraro PA, Nicholas R, Roncaroli F, Reynolds R. Meningeal inflammation plays a role in the pathology of primary progressive multiple sclerosis. Brain 2012;135(10):2925–37.

16. Frischer JM, Bramow S, Dal-Bianco A, Lucchinetti CF, Rauschka H, Schmidbauer M, Laursen H, Sorensen PS, Lassmann H. The relation between inflammation and neurodegeneration in multiple sclerosis brains. Brain 2009;132(5):1175–89.

17. Magliozzi R, Howell O, Vora A, Serafini B, Nicholas R, Puopolo M, Reynolds R, Aloisi F. Meningeal B-cell follicles in secondary progressive multiple sclerosis associate with early onset of disease and severe cortical pathology. Brain;130(4):1089–104.

18. Bø L, Vedeler C, Nyland H, Trapp B, Mørk S. Intracortical multiple sclerosis lesions are not associated with increased lymphocyte infiltration. Mult Scler 2003;9(4):323–31.

19. Peterson JW, Bö L, Mork S, Chang A, Trapp BD. Transected neurites, apoptotic neurons, and reduced inflammation in cortical multiple sclerosis lesions. Ann Neurol 2001; 50(3):389–400.

20. Guseo a, Jellinger K. The significance of perivascular infiltrations in multiple sclerosis. J Neurol 1975;211(1):51–60.

21. Kutzelnigg A, Lucchinetti CF, Stadelmann C, Brück W, Rauschka H, Bergmann M, Schmidbauer M, Parisi JE, Lassmann H. Cortical demyelination and diffuse white matter injury in multiple sclerosis. Brain 2005; 128(11):2705–12.

22. Serafini B, Rosicarelli B, Magliozzi R, Stigliano E, Aloisi F. Detection of Ectopic B-cell Follicles with Germinal Centers in the Meninges of Patients with Secondary Progressive Multiple Sclerosis. Brain Pathol 2004;14(2):164–74.

23. Lassmann H, Brück W, Lucchinetti CF. The immunopathology of multiple sclerosis: an overview. Brain Pathol 2007;17(2):210–8.

24. Howell OW, Reeves CA, Nicholas R, Carassiti D, Radotra B, Gentleman SM, Serafini B, Aloisi F, Roncaroli F, Magliozzi R, Reynolds R. Meningeal inflammation is widespread and linked to cortical pathology in multiple sclerosis. Brain 2011; 134(9):2755–71.

25. Magliozzi R, Howell OW, Reeves C, Roncaroli F, Nicholas R, Serafini B, Aloisi F, Reynolds R. A Gradient of neuronal loss and meningeal inflammation in multiple sclerosis. Ann Neurol 2010; 68(4):477–93.

26. Law AJ, Harrison PJ. The distribution and morphology of prefrontal cortex pyramidal neurons identified using anti-neurofilament antibodies SMI32, N200 and FNP7. Normative data and a comparison in subjects with schizophrenia, bipolar disorder or major depression. J Psychiatr Res;37(6):487–99.

27. Gardner C, Magliozzi R, Durrenberger PF, Howell OW, Rundle J, Reynolds R. Cortical grey matter demyelination can be induced by elevated pro-inflammatory cytokines in the subarachnoid space of MOG-immunized rats. Brain 2013; 136(12):3596–608.

28. Dal Bianco A, Bradl M, Frischer J, Kutzelnigg A, Jellinger K, Lassmann H. Multiple sclerosis and Alzheimer's disease. Ann Neurol 2008; 63(2):174–83.

29. Corcione A, Casazza S, Ferretti E, Giunti D, Zappia E, Pistorio A, Gambini C, Mancardi GL, Uccelli A, Pistoia V. Recapitulation of B cell differentiation in the central nervous system of patients with multiple sclerosis. Proc Natl Acad Sci U S A 2004; 101(30):11064–9.

30. Obermeier B, Mentele R, Malotka J, Kellermann J, Kümpfel T, Wekerle H, Lottspeich F, Hohlfeld R, Dornmair K. Matching of oligoclonal immunoglobulin transcriptomes and proteomes of cerebrospinal fluid in multiple sclerosis. Nat Med 2008;14(6):688–93.

31. Torkildsen Ø, Stansberg C, Angelskår SM, Kooi E-J, Geurts JJG, van der Valk P, Myhr KM, Steen VM, Bø L. Upregulation of immunoglobulin-related genes in cortical sections from multiple sclerosis patients. Brain Pathol 2010; 20(4):720–9.

32. Calabrese M, Federle L, Bernardi V, Rinaldi F, Favaretto A, Varagnolo MC, Perini P, Plebani M, Gallo P. The association of intrathecal immunoglobulin synthesis and cortical lesions predicts

disease activity in clinically isolated syndrome and early relapsing-remitting multiple sclerosis. Mult Scler 2012; 18(2):174–80.

33. Disanto G, Morahan J., Giovannoni G, Ramagopalan S. The evidence for a role of B cells in multiple sclerosis. Neurology. 2012;78:823–32.

34. Lawrie S, Bar-Or A. B cells set trends: Lessons from multiple sclerosis. Clin Exp Neuroimmunol 2012; 3(3):89–108.

35. Lisak RP, Benjamins J a, Nedelkoska L, Barger JL, Ragheb S, Fan B, Ouamara N, Johnson TA, Rajasekharan S, Bar-Or A. Secretory products of multiple sclerosis B cells are cytotoxic to oligodendroglia in vitro. J Neuroimmunol 2012; 246(1-2):85–95.

36. Qin Y, Duquette P, Zhang Y, Olek M, Da R, Richardson J, Antel JP, Talbot P, Cashman NR, Tourtellotte WW, Wekerle H, Van Den Noort S. Intrathecal B-Cell Clonal Expansion, an Early Sign of Humoral Immunity, in the Cerebrospinal Fluid of Patients with Clinically Isolated Syndrome Suggestive of Multiple Sclerosis. Lab Investig 2003; 83(7):1081–8.

37. Cross AH, Stark JL, Lauber J, Ramsbottom MJ, Lyons J-A. Rituximab reduces B cells and T cells in cerebrospinal fluid of multiple sclerosis patients. J Neuroimmunol 2006; 180(1-2):63–70.

38. Bar-Or A, Fawaz L, Fan B, Darlington PJ, Rieger A, Ghorayeb C, Calabresi PA, Waubant E, Hauser SL, Zhang J, Smith CH. Abnormal B-cell cytokine responses a trigger of T-cell-mediated disease in MS? Ann Neurol 2010; 67(4):452–61.

39. Kurtzke JF, Beebe GW, Nagler B, Kurland LT, Auth TL. Studies on the natural history of multiple sclerosis—8. J Chronic Dis 1977; 30(12):819–30.

40. Calhoun ME, Jucker M, Martin LJ, Thinakaran G, Price DL, Mouton PR. Comparative evaluation of synaptophysin-based methods for quantification of synapses. J Neurocytol 1996; 25(12):821–8.

41. Kemp K, Gray E, Wilkins A, Scolding N. Purkinje cell fusion and binucleate heterokaryon formation in multiple sclerosis cerebellum. Brain 2012; 135(10):2962–72.

42. Shields SD, Cheng X, Gasser A, Saab CY, Tyrrell L, Eastman EM, Iwata M, Zwinger PJ, Black JA, Dib-Hajj SD, Waxman SG. A channelopathy contributes to cerebellar dysfunction in a model of multiple sclerosis. Ann Neurol 2012; 71(2):186-94.

43. Junker A, Brück W. Autoinflammatory grey matter lesions in humans: Cortical encephalitis, clinical disorders, experimental models. Curr Opin Neurol 2012; 25(3):349–57.

Figure 1. Demyelination is increased in lymphoid-like positive SPMS. MOG immunohistochemistry revealed areas of cerebellar demyelination. Lesions (A, arrowheads) often surrounded infoldings of the cerebellar folia (asterisk). Myelin, normally present in the granule cell layer (GCL), and the Purkinje cell layer of the cerebellar grey matter in control (B), was absent in demyelinated lesions of SPMS cases (C). Demyelination predominantly affected the grey matter and in some instances subpial lesions could be seen to extend into the white matter (D, arrowheads). Colour masks (E) were applied to highlight areas of white and grey matter lesions for quantification (F-H). Grey matter demyelination varied markedly between cases (F-H; corresponding to MS204, MS224 and MS217, respectively). Total demyelination (as a percentage of the total area assessed), the proportion of cerebellar cortical white matter and the proportion of grey matter demyelination were greater in cases previously characterised by the presence of forebrain lymphoid-like structures (F+) in comparison to F-SPMS (I). Note that four F- SPMS and two F+ SPMS cases did not present with demyelinated plaques in the samples analysed and are not included in this analysis. Kruskal-Wallis and Dunn's multiple comparisons post-test, group medians and interquartile range shown. Cases with the most extensive cerebellar grey matter demyelination also had the greatest proportion of demyelinated forebrain cortical grey matter, indicating a widespread association between meningeal inflammation and subpial grey matter pathology in progressive MS (J). F+ SPMS cases are identified as red data points. Spearman (non-parametric) comparison. GCL, granule cell layer; GML, grey matter lesion; ML, Molecular layer; WML, white matter lesion; F+/-, lymphoid-like status positive/negative. Scale bars: A) 1 mm; B- D) 200 µm; F- H) 1.5 cm.

Figure 2. Diffuse cellular infiltrates of the cerebellar meninges. Tissue blocks were rated for meningeal inflammation based on number and organisation of haematoxylin stained inflammatory infiltrates. A rating of 0+ referred to fewer than 10 cells per area of interest (A), accumulations of between 10-30 cells (+)(B), > 30 cells in a loose or disorganised aggregate (++)(C), whilst >100 cells in

a tightly packed aggregate were rated as (+++)(D). An example of a (+++) aggregate in the cerebellar meninges of MS257 with a core of B-cells (E - CD20+ immunohistochemistry, and inset showing CD20+ B-cells and nuclear haematoxylin stain taken from a separate +++ meningeal aggregate from the same case), and surrounded by T-cells (F, CD3+ blue immunoprecipitate) and plasma cells (G, immunoglobulin A+,G+,M+). A far more frequent finding was that of smaller and less dense cellular aggregates lacking organisation (rated ++) in the cerebellar meninges consisting of macrophages (H), B-cells (I), and CD4+ (J) and CD8+ T-cells (K) taken from the F- SPMS case MS395. Scale bars: A) 250 µm; B) 80 µm; C) 150 µm.

Figure 3. Quantifying meningeal cerebellar inflammation. Regions of interest of the cerebellar meninges and Purkinje cell layer were identified from two areas of normal appearing and two areas of demyelinated grey matter per case (A). Quantification of meningeal CD20+ B-cells (B) and immunoglobulin A+, G+, M+ meningeal plasma cells (C) revealed their number to be significantly increased in F+ SPMS in comparison to controls. Note that one F- SPMS case was removed from the analysis (MS355) as a statistically significant outlier (Grubbs test; $z=3.49$, $p<0.01$) with a value 11 fold greater than the group median. The number of CD68+ macrophages was increased in both F+ and F- SPMS (D) in comparison to controls, whilst the number of CD4+ (F), but not CD8+ (G) T-lymphocytes was significantly increased in F+ SPMS in comparison to the other groups. Group medians (and interquartile range) were compared by Kruskal-Wallis and Dunn's post-test.

Figure 4. Lymphoid-like positive secondary progressive MS cases exhibit increased parenchymal inflammation. CD68+ cells with a process-bearing microglia morphology, and others with a rounded and more darkly stained macrophage morphology, were seen in elevated numbers in the molecular and Purkinje cell layers of F+ SPMS (B, MS278; D, MS212) in comparison to controls (A, C044). Quantification of CD68+ cell densities in the grey matter parenchyma revealed a significant increase in CD68+ microglia/macrophages in the F+ SPMS cohort in comparison to control and F- SPMS (C).

Group medians (and interquartile range) were compared by Kruskal-Wallis and Dunn's post-test. Ctrl, control cases; SPMS, secondary progressive multiple sclerosis. Scale bar: 100 µm.

Figure 5. Purkinje cell degeneration is not a feature of progressive MS. Non-phosphorylated neurofilament immunostained section (A, and inset) illustrating the distribution of Purkinje cells in a control case. Purkinje cell density was determined for SPMS and control cases and was not different between groups (B), although those SPMS cases characterised by forebrain lymphoid-like structures showed a trend to a reduced number of Purkinje cell neurons. Group medians (and interquartile range) were compared by Kruskal-Wallis and Dunn's post-test. C) Calbindin immunohistochemistry revealed the occasional Purkinje cell axon with distinctive end-bulb pathology (arrow, MS352). Synapse density was quantified in the molecular layer (ML) and the granule cell layer (GCL) of synaptophysin immunostained sections (D) and was not altered between control and disease. PCL, Purkinje cell layer; SPMS, secondary progressive multiple sclerosis. Scale bars: A) 250 µm; inset) 50 µm; C, D) 60 µm.

Table 1. Summary of clinical data

Cases	Number of cases	Females	Age at disease onset	Age at death	Disease duration	Post-mortem delay
Controls	11	8	-	66.5 (35 – 84)	-	21.5 (5 - 33)
F+ SPMS cases	12	10	27.3 (9 – 42)	49.75 (30 – 61)	22.4 (6 – 40)	35.1 (9 - 66)
F- SPMS cases	15	9	31 (19 – 56)	56.4 (46 – 64)	25.4 (15 – 39)	20.8 (4 - 44)

Age at onset, age at death and disease duration in years. Post-mortem delay in hours. F+, F- SPMS refers to those secondary progressive MS cases characterized as harboring B cell follicle lymphoid-like structures in the forebrain meninges (24). Values indicate group means, with the data range given in brackets.

Table 2. Primary antibodies and antigen retrieval conditions.

Target Cell/Molecule	Antigen	Antigen retrieval buffer	Antibody Source	Clone
Myelin oligodendrocyte glycoprotein	MOG	0.01M Citrate buffer	In house	Z12
Activated microglia and macrophages	CD68	0.01M Tris + EDTA	Dako, CA, USA	Cr3/43
B-cells	CD20	0.01M Tris + EDTA	Invitrogen, Carlsbad, CA	L26
CD4+ T-cells	CD4	0.01M Tris + EDTA	Abcam, Cambridge, UK	BC/1F6
CD8+ T-cells	CD8	0.01M Tris + EDTA	Dako	C8/144B
Plasma cells	IgG/A/M	0.01M Tris + EDTA	Dako	Polyclonal
Purkinje cells	non-phosphorylated neurofilament H	0.01M Citrate buffer	Abcam	Smi-32
Purkinje cell neurites	Calbindin	0.01M Citrate buffer	Sigma-Aldrich, Dorset, UK	CL-300
Synapses	Synaptophysin	0.01M Citrate buffer	Dako	Polyclonal

Table 3. Association between meningeal inflammation and underlying cerebellar grey matter pathology.

	CD68+ monocytes	CD4+ T cells	CD8+ T cells	CD20+ B cells	Ig+ Plasma cells	CD68+ microglia
CD4+ T cells	0.42 *					
CD8+ T cells	0.31	0.41 *				
CD20+ B cells	0.41 *	0.36	0.41 *			
Ig+ Plasma cells	0.24	0.3	0.24	0.32		
CD68+ microglia	0.54 **	0.06	0.11	0.28	0.04	
Area of GML	0.3	0.37	0.35	0.35	0.48 *	0.45 *

Spearman rank correlation analysis comparing inflammatory cell densities of the meninges and parenchymal microglial activation and extent of cerebellar cortex demyelination. Spearman r values are shown and significant associations are noted by asterisks. *, $p<0.05$; **, $p<0.01$ and exact p values quoted in the text.

Figure 1

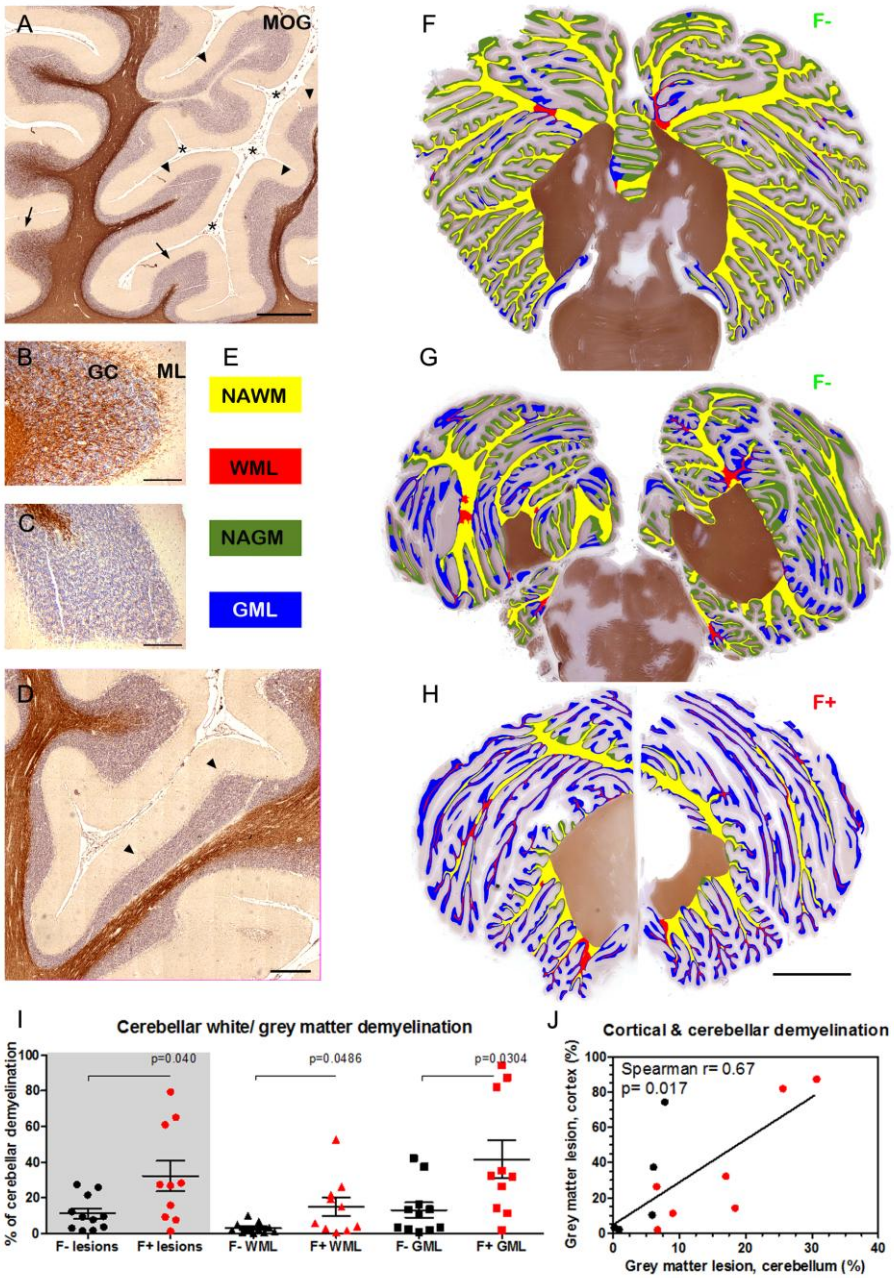

NAN_12199_F1

Figure 2

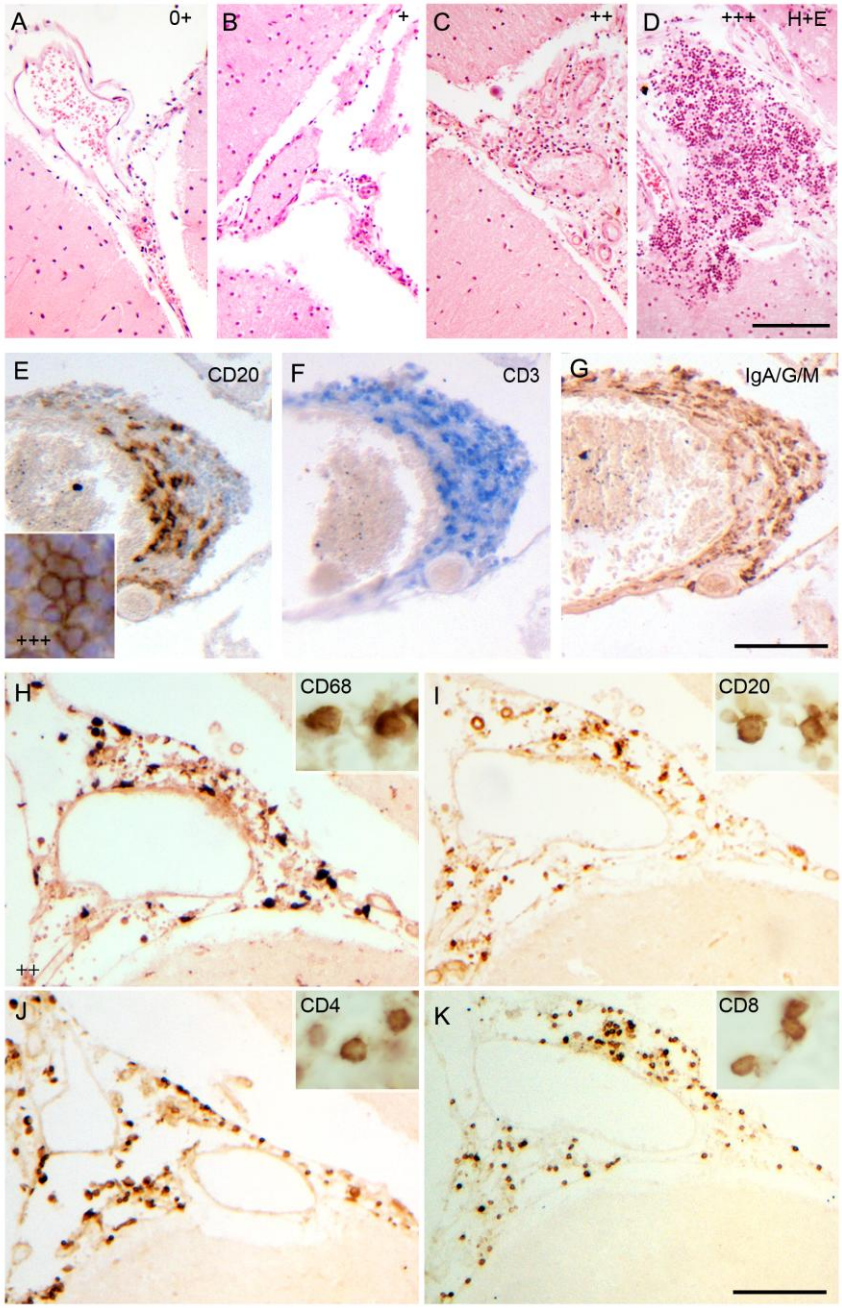

NAN_12199_F2

Figure 3

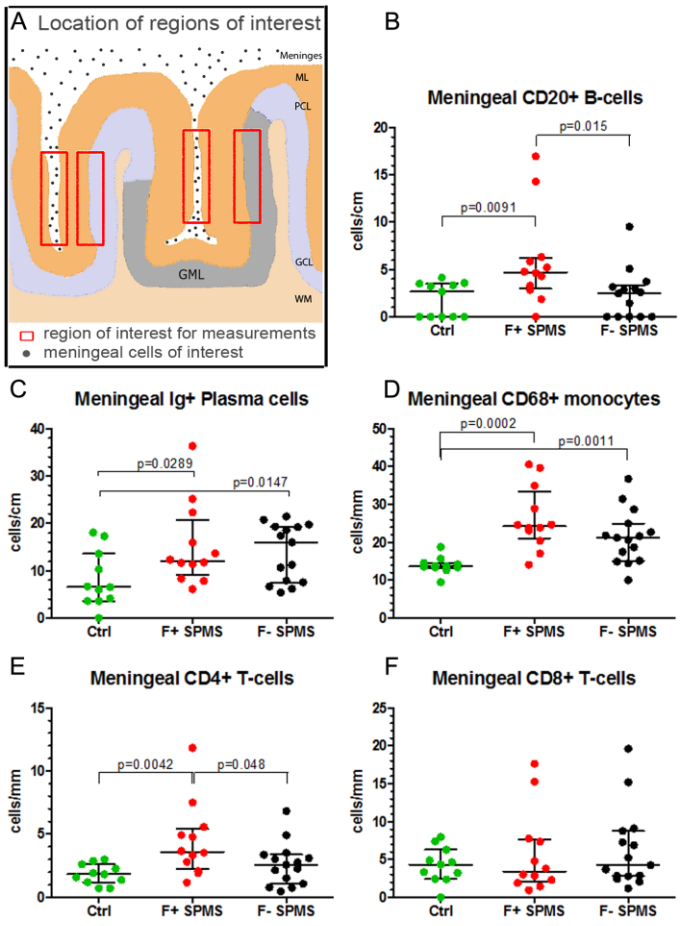

NAN_12199_F3

Figure 4

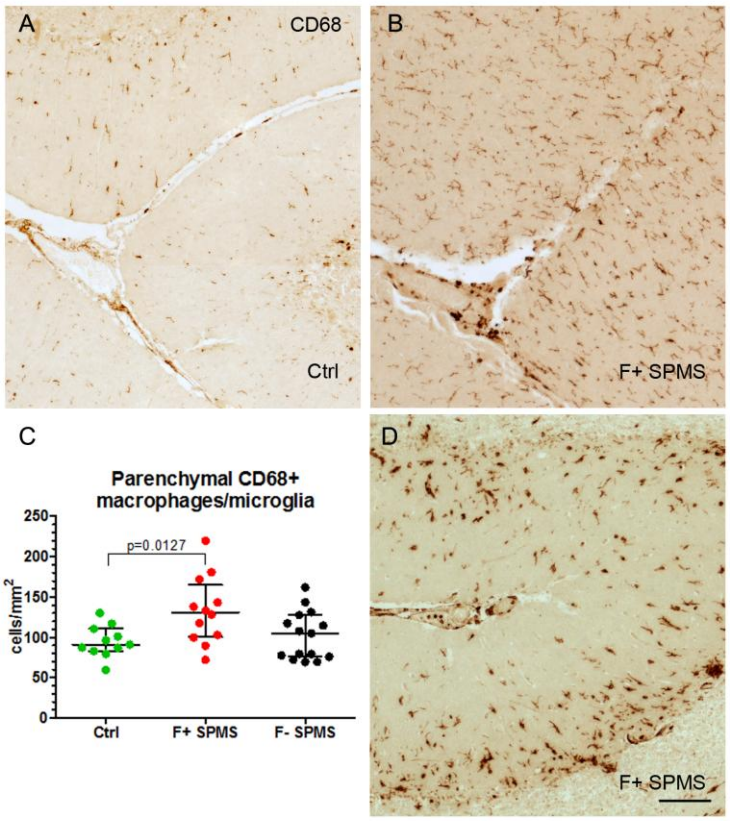

NAN_12199_F4

Figure 5

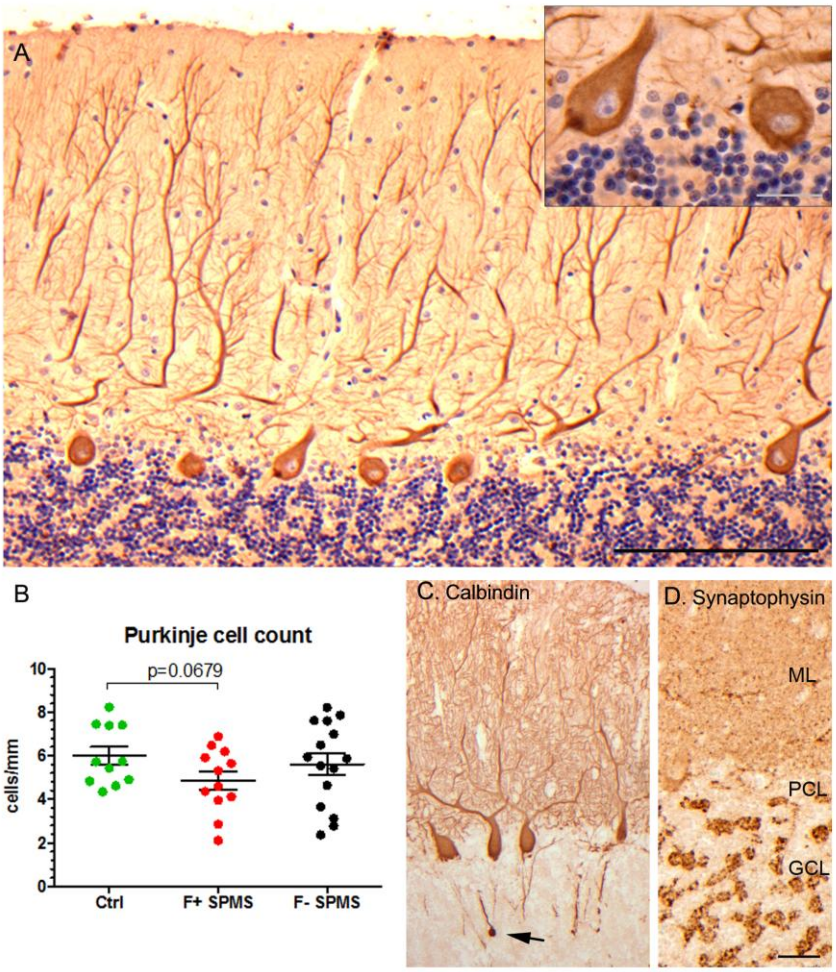

NAN_12199_F5